Design and Synthesis of 3-D Reduced Graphene Oxide Foam for High-performance Supercapacitor Electrodes

参赛队员姓名： 洪润楠

中学： 华南师范大学附属中学

省份： 广东省

国家/地区： 中国

指导老师姓名： 邓达义副教授、杨晓安

指导老师学校： 华南师范大学、华南师范大学附属中学

Statement of Originality

This study was carried out by Runnan Hong under the guidance of Mr. Yang and Prof. Deng. The paper is original, with proper citations to literature studies. The paper has not been submitted for any publication either.

Team Member Signature:

Instructor Signature:

Date: 2020-9-13

Design and Synthesis of 3-D Reduced Graphene Oxide Foam for High-performance Supercapacitor Electrodes

Team Member

Runnan Hong

Instructor

Prof. Dayi Deng from South China Normal University, Xiaoan Yang from the Affiliated High School of South China Normal University

School

The Affiliated High School of South China Normal University

Location

Guangzhou, Guangdong, P.R. China

华南师范大学附属中学
The Affiliated High School of SCNU

Abstract:

Graphene is a single layer (monolayer) of sp^2-bonded carbon atoms bound in a hexagonal honeycomb lattice. Due to its exceptional high surface area and electric conductivity, graphene has been widely applied as a proposing electrode material of electric double-layer supercapacitors. During the preparation of supercapacitors, dispersed reduced graphene oxide (RGO) or graphene oxide (GO) is often loaded onto a support skeleton through dip-coating method. RGO and GO sheets are highly susceptible to restacking due to π-π interaction, which may substantially reduce the accessible surface and consequently the double-layer effect. To address the above issue, a new synthetic route was designed and established for the preparation of 3-D graphene porous supercapacitor material. First, commercial melamine foam was carbonized at 800 °C under ultrapure N_2 atmosphere to produce nitrogen-rich porous carbon foam (NCF) as the support skeleton. GO sheets and dopamine (DA) hydrochloride were dissolved in water, and readily dispersed into the 3-D pore structure of NCF. When heated to 60 °C, GO and DA crosslinked together and formed a stable hydrogel that kept GO sheets dispersed and limited the restacking of GOs. Thereafter, the GO loaded NCF underwent calcination under ultrapure N_2 atmosphere at 800 °C to produce RGO loaded NCF (RGO-NCF). Following KOH activation by annealing the RGO-NCF at 800 °C under ultrapure N_2 atmosphere significantly improve the specific capacitance, due to substantial increase in the specific surface of KOH-RGO-NCF. During the study, the impact of calcination temperature, GOs concentration and DA concentration on the electrochemical properties of the resulting KOH-RGO-NCF was elucidated to optimize the preparation conditions. Under the optimized conditions, the resulting KOH-RGO-NCF has a large specific area (1,555 m^2/g) and a capacitance of 171.6 F/g at a scan rate of 5 mV/s in 1 M Na_2SO_4 aqueous solution. SEM analysis shows that the resulting KOH-RGO-NCF has 3-D pore structure with RGO sheets dispersed in the pore space. As a result, the restacking issue can be minimized through optimization of the ratios and concentrations of GO and DA; further electrochemical tests confirm that KOH-RGO-NCF has ideal double-layer behaviors. Overall, this study offers a promising approach to overcome the restacking issue of RGOs/GOs sheets, and fabricate porous nitrogen-rich carbon supported 3-D reduced graphene oxide foam as high-performance electrodes for electric double-layer supercapacitors.

CONTENT

1. Introduction

### 1.1 Overview of supercapacitors

Electric energy storage technologies are generally divided into two categories, the physical energy storage technology and the chemical energy storage. The chemical energy storage technology can be further classified into the battery technology and the supercapacitor technology. A supercapacitor has two conducting surfaces, and energy is stored on these surfaces. These conductive surfaces act as the electrodes of a supercapacitors.[1]

Supercapacitors have high power density with long-cycle life, which can complement conventional batteries. They have many favorite features, include light-weight, fast charging, high discharge performance, wide operating temperature range, etc.[1] In addition, they are maintenance-free and non-hazardous. They can be used as a stand-alone power supply or duplex power supply. Because of their superior features of long service life and high-power density performance, supercapacitors have broad potential application in mobile multimedia equipment, renewable energy production, aerospace systems, transportation systems and other fields.[2]

1.2 The basic principles and the classification of supercapacitors

According to the energy storage mechanism, supercapacitors can be divided into two categories, the double-layer capacitor and the pseudocapacitor.[3] The concept of a double-layer was first proposed by German physicist Helmholtz in the 19th century when he studied the opposite charges at the interfaces of colloidal particles. The working principles of double-layer capacitors are illustrated in Scheme 1. When a pair of electrodes are immersed in the electrolyte and connected to external electric field, positive charges and negative charges are arranged into two ion layers at the electrode/electrolyte interface, due to electrostatic interaction of these two charged species.[3] When the external circuit is disconnected, the double-layers between the electrode and the electrolyte will be maintained, which thus generates a relatively stable voltage. During the process of discharge, the reverse processes happen. As double-layer capacitors

1

store or release energy only through physical processes without electrochemical reactions occurring, they generally have high cycle stability and a fairly long service life.[3]
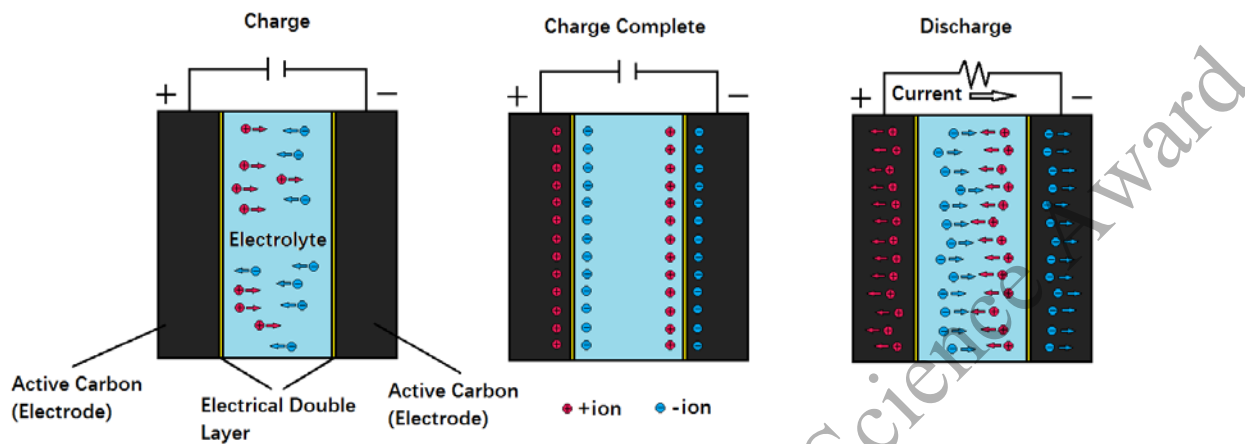
Scheme 1. The working principle of double-layer capacitors

The selection of electrode materials directly determines the electrical performances of the supercapacitors, as the double-layer effect is key to the charge and discharge processes. Porous carbon materials have large specific surface areas and high energy density.[4, 5] They are highly electric conductive, with well-developed mesoporous structures that facilitate electronic transmission and electrolyte diffusion. Porous carbon materials also have excellent physical and chemical stability. Because of these favorite features, porous carbon materials have been often utilized as the electrode materials for the fabrication of double-layer supercapacitors.[4, 5]

Pseudocapacitors, also known as Faraday pseudocapacitor, rely on rapid reversible redox reactions of electrolyte ions on the electrode surface and the bulk liquid phase to store and release energy.[6] This feature is similar to that of the secondary battery (the charge battery). However, the redox reactions involved in the charge and discharge processes of pseudocapacitors are reversible, which differ from those of secondary batteries. The redox reactions of pseudocapacitors also proceed much more rapidly than those of the latter ones. The potential of the electrode is constantly changing during the charge and discharge processes. Hence, pseudocapacitors has no charging and discharge platform, as double-layer capacitors do.[7] During the

charging period, a large number of electrolyte anions and cations are transferred from the electrolyte solution to the electrode/electrolyte interface, and rapid electrochemical reactions occur at the interface. When the external circuit is disconnected, a large number of cations and anions are instantly transferred from the electrode back into the electrolyte bulk phase, and the charge stored between the two electrodes is finally released from the external current in the form of discharge electricity. Pseudocapacitor generally have high energy density. However, the cycle-life of pseudocapacitors is low, as chemical reactions are involved in the charge and discharge processes.[7] In addition, pseudocapacitors are generally constructed of water-based electrolyte systems, which have limited operating voltages and consequently low energy density. Due to the above shortcomings of pseudocapacitors, double-layer supercapacitors have higher potential of practical application.[2]

Hybrid supercapacitors are a newly developed class of asymmetric hybrid capacitors. Unlike symmetric capacitors, the anode electrode and cathode electrode are made of pseudocapacitance materials and double-layer materials, respectively. The anode electrode is generally constructed of transition metal oxides that can participate in Faradaic redox reactions, and the materials generally have high specific capacitance and specific energy. The cathode materials are often carbon materials of large specific surface areas for increased double-layer effect. Hybrid capacitors have both favorite features of the pseudocapacitor and the double-layer capacitors, including high specific energy and long-cycle life of both capacitors and double-layer capacitors.[3]

1.3 Overview of compressible supercapacitors

In order to power wearable electronic devices and soft robots, it is necessary to develop highly compressible energy supply devices that are different from conventional energy supplies.[8] Research on compressible capacitors focuses on high-performance compressible electrodes, which fall into two main categories: (1) self-supporting carbon foam electrodes (e.g. carbon nanotubes, graphene), as well as composite materials consisting of these carbon foams, conductive polymers and metal oxides,[9, 10] and (2) electrodes

3

composed of compressible supports (e.g. polyurethane foams, cellulose aerogels) loaded with active substances.[11] Compressible carbon foam supercapacitors are mostly constructed of graphene, carbon nanotube aerogels or chemical gas deposition carbon foams.[12-15] Self-supporting carbon foam electrodes generally have good electrochemical properties, because carbon foam materials are highly electric-conductive. However, carbon foam electrode may suffer from poor mechanical properties, due to the lack of skeleton support. Compared with carbon foam materials, cellulose aerogels and polyurethane foams have higher mechanical robustness, but they are not electric-conductive.

1.4 Motivation and aim of this study

Prior to the discovery of graphene, carbon materials, especially activated carbon, had been used in commercial supercapacitors. Activated carbons are chosen as the electrode materials of supercapacitors, due to their favorite features, including large specific surface areas, electric conductivity, chemical stability. [2] In comparison, graphene, consisted of a single layer of sp^2 carbon atoms, has much greater electric conductivity than conventional carbon materials. Literature study show that a single layer of graphene has a specific capacitance of $20\mu F/cm^2$.[16] Graphene has a theoretical specific capacitance of 550 F/g, higher than other carbon materials.[17] Graphene has extremely high specific surface area (2630 m^2/g),[17] and the layered structure of graphene electrodes offers abundant accessible channels for the migration and diffusion of electrolyte ions. In an ideal state, single-layer graphene also has a high field modality and excellent fracture strength. Due to the above mentioned favorite features, graphene has been deemed a promising supercapacitor electrode material with exceptional specific energy.[18-20]

Many researchers have tested the application of graphene as supercapacitor electrodes in the last decades.[17] In the preparation of graphene electrode materials for supercapacitors, chemical oxidation methods are generally first applied to obtain graphene oxide (GO), and then reduced graphene oxide (RGO) is produced through reduction treatment of GO.[17, 21] For example, Stoller et al. produced reduced graphene oxide (RGO) as electrode material of supercapacitors through chemical reduction of graphene oxide (GO), and the specific capacitance of the RGO electrodes in KOH aqueous systems and organic

4

systems are 135 F/g, and 99 F/g, respectively.[22] Yu at al. used NaBH$_4$ to reduce the GO film obtained after vacuum filtration, producing RGO film as supercapacitor electrode materials with a specific capacitance of 135 F/g in 2 M KCl electrolyte aqueous solutions.[23]

During reduction treatment, oxygen-containing function groups of GOs are gradually removed, hence decreasing the Coulomb repulsion between GO/RGO sheets. In addition, GO/RGO sheets can restack together through π-π interactions, as GO and RGO are consisted of a single layer of overlapping sp^2 hybrid bonds.[17] Unfortunately, these factors render the restacking and coalescing phenomena of RGO sheets, which may seriously reduce the accessible surface area, the electric conductivity and specific capacitance of the RGO sheets.[18] Thus, how to minimize the restacking of GO sheets and RGO sheets is critical for the fabrication of high-performance graphene supercapacitors.[17]

Three-dimensional (3-D) graphene offers a potential solution to the above issue.[19] Xu et al. prepared 3-D porous graphene through one-step hydrothermal synthesis.[24] Their results indicate that the 3-D pore structure of the material can prevent restacking of graphene, and consequently increase the specific capacitance to 165 F/g.[24] However, the mechanical robustness of 3-D graphene materials is often poor, because there is no skeleton support.[17] To address the above issue, researchers tested the utilization of porous foams as the support skeleton of graphene in recent years, and prepared compressible graphene foam composite supercapacitor material.[25] During the synthesis, GO sheets are often dispersed within the 3-D porous structure of carbon foams by simple dip-coating, followed by conventional chemical reduction or calcination to reduce GOs.[26] 3-D composite electrode materials prepared through such simple dip-coating method often have low loading of graphene and consequent low volumetric capacitance. Most importantly, the above preparation process is still difficult to avoid the restacking phenomena of graphene.

Against the above background, this study aimed to address the restacking issue of graphene, and developed a new synthesis process for the preparation of porous carbon foam supported 3-D compressible graphene foam as electrode materials of supercapacitors. In this study, nitrogen-rich 3-D porous carbon

foams derived from calcination of commercial melamine foams are utilized as the support skeleton for graphene, and the carbonization process is simple and convenient as outlined in Scheme 2. Nitrogen-rich 3-D porous carbon foams derived from melamine are known to have high electric conductivity, exceptional mechanical strength and good compressible elastic property.[25] In addition, the nitrogen doping can improve the hydrophilic property of the skeleton, which facilitates the migration and diffusion of electrolytes.[26] All these features make nitrogen-rich 3-D porous carbon foams an ideal support skeleton of graphene.
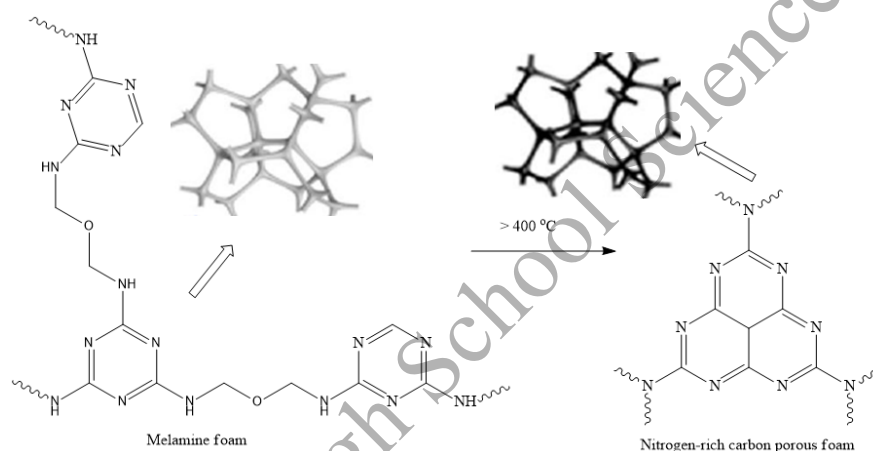
Scheme 2. Synthesis of nitrogen-rich porous carbon foams from melamine foams

Dopamine, a biomimetic adhesive molecule, is applied to disperse and anchor GO sheets into the pore structure of the nitrogen-rich 3-D porous carbon foam. Dopamine and GO sheets are dissolved in aqueous solutions, and dispersed in the pore structure of the 3-D porous foam. When heated to about 60 °C under steady conditions, dopamine and GO sheets can form stable hydrogel,[27] which facilitates anchoring and dispersing GO sheets into the 3-D pore structure. More importantly, dopamine molecules can cross-link GO sheets through electrostatic force as well as forming covalent bonds between these two species.[28] This can space GO sheets away from each other and limit the restacking of GO sheets, as illustrated in Scheme 3. In addition, the dopamine composition in the hydrogel has a chemical composition similar to the adhesive material secreted by mussels, and may adhesive on the surface of the skeleton support. Dopamine

6

can partially reduce the GO sheets as well.[29] Carbonization of the composite materials at high temperature can further improve reduction GO sheets to RGO sheets. During the carbonization treatment, dopamine/polydopamine can be carbonized into nitrogen-doped graphene-like material at high temperature as well.[30] Through such loading process, it may be feasible to load the pores of the 3-D nitrogen-rich porous carbon foams with high density of graphene/graphene-like materials while minimizing potential restacking of RGO sheets. Finally, the composite material is activated by KOH annealing at high temperature to increase the formation of meso/micro pores, which can substantially increase the specific surface areas and electrochemical performance of the materials.[31] Overall, this study offers an simple solution to the restacking issue of GO and RGO sheets, and develops a promising process for the fabrication of 3-D porous nitrogen-rich carbon supported reduced graphene oxide foam as high-performance supercapacitor electrodes.
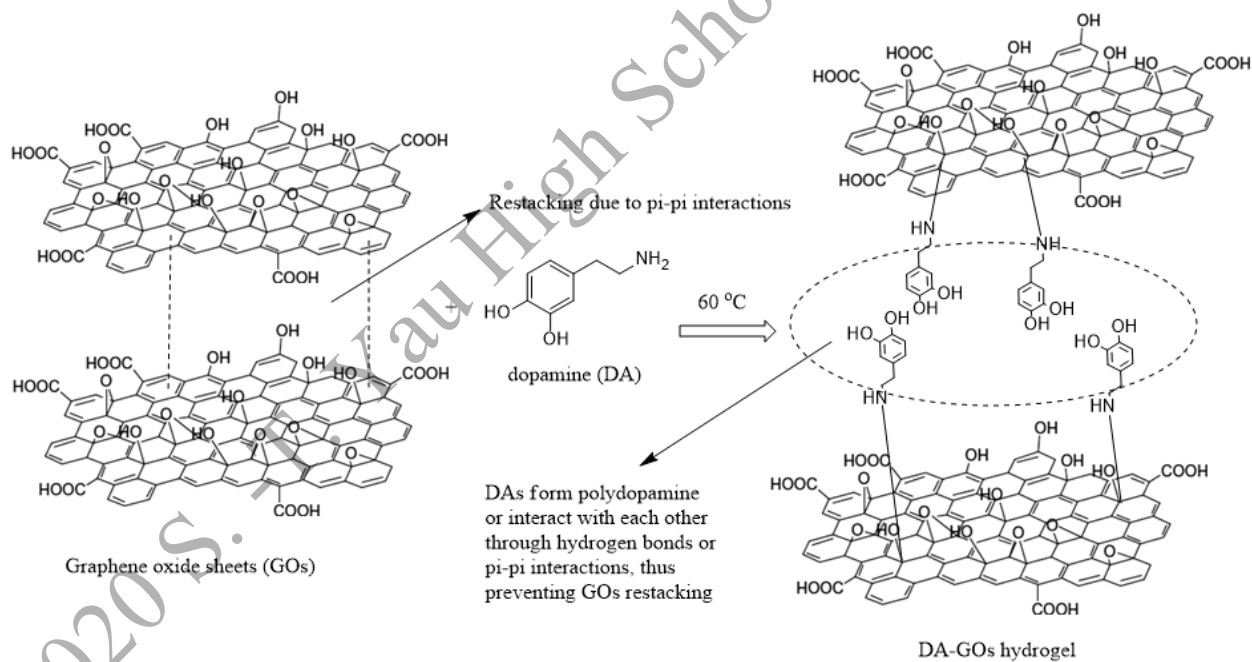
Scheme 3. The mechanism of preventing GOs restacking with dopamine

2. Materials and Methods

2.1 Materials

7

Commercial melamine foam was from Beijing Kelinmei Co. Ltd. Ultrapure graphene oxide (GO) was purchased from Suiheng Technology Co. Ltd. Absolute ethanol, sulfuric acid, ammonia solution, dopamine (DA) hydrochloride, potassium hydroxide, and sodium sulfate were analytical grade. All aqueous solutions were prepared with deionized water (~18MΩ·cm).

2.2 Fabrication of 3-D porous nitrogen-rich carbon foams

A piece of commercial melamine foam (2cm $\times$ 4cm $\times$ 4cm) was washed with DI water and absolute ethanol alternatively for three times. The foam block was then blow-dried in an oven at 60 °C. The block was then added into a in a porcelain boat, and then heated in a tube furnace under an atmosphere of ultrapure N_2 gas (99.9999%) at 5 °C /min. After reaching the designated carbonization temperature (600 °C, 800 °C, 900 °C), the sample was carbonized at the set temperature for 2 h, followed by naturally cooling down to room temperature. The resulting nitrogen-rich porous carbon foam was then immersed and cleaned in DI water, followed by blow-dry in an oven at 60 °C.

Designated amount of GO sheets (1.0 g/L, 2.0 g/L or 10.0 g/L) was ultrasound-dispersed in 100 mL DI water for 10 min in an ultrasonic cleaner. The pH of dispersed GO solution was adjusted to 7 by adding dilute ammonia solution. Thereafter, designated amount of DA hydrochloride was added into the GO solutions, and the final concentrations of DA hydrochloride in the resulting solutions were 0.1 g/L, 0.5 g/L, 1.0 g/L and 5.0 g/L, respectively. Nitrogen-rich porous carbon foam was then immersed into the resulting solutions, and squeezed several times to remove the air inside the foam. Thereafter, the flask containing the solution and the immersed foam were heated at 60 °C without stirring for 6 h for the formation of hydrogel. Thereafter, the immersed foam filled with hydrogel inside its pore structure was taken out, and blow-dried at 60 °C.

The dried foam loaded with GOs and DA was then carbonized at designated temperature (600 °C, 800 °C, and 900 °C). The carbonization and sample workup procedures were basically the same as those for the carbonization of the commercial melamine foam. The resulting foam was immersed and squeezed several

times in 20 mL of KOH aqueous solution, and the weight ratio of KOH/foam was 3:1.[32] The foam loaded with KOH solution was then dried at 60 °C. Thereafter, the dried KOH-loaded foam was activated at designated temperature (600 °C, 800 °C, and 900 °C) in the tube furnace. The heating procedures were basically as those for the carbonization of commercial melamine foams. The final activated foam was washed with dilute HCl solution and then DI water, and blow-dried at 60 °C.[32]

During the study, nine different electrode foam materials were prepared to optimize the preparation conditions for the fabrication of 3-D reduced graphene foam with high electrochemical performance. Thus, the impact of carbonization temperature and annealing temperature, the concentrations of GO and the concentrations of DA on the structure and electrochemical properties of the foam materials were studied. The preparation conditions and the label for the nine foam materials were summarized in Table 1.

Table 1. Preparation conditions and labels of the resulting foams

Foam Label	Melamine carbonatization temperature (°C)	GO (g/L)	Dopamine hydrochloride (g/L)	Carbonization temperature of GO loaded foam (°C)	KOH activation temperature (°C)
800	800	-	-	-	-
800-2-1	800	2	1	800	-
800-2-1-800-800	800	2	1	800	800
800-10-1-800-800	800	10	1	800	800
800-10-5-800-800	800	10	5	800	800
800-2-0.1-800-800	800	2	0.1	800	800
800-2-0.5-800-800	800	2	0.5	800	800
600-2-1-600-600	600	2	1	600	600
900-2-1-900-900	900	2	1	900	900

2.3 Material characterization

Morphological analysis of the samples was conducted by scanning electron microscopy (SEM) using a Hitachi 4700 microscope. Specific surface area (SSA) of the foams were determined by nitrogen adsorption using the Brunauer–Emmett–Teller (BET) method (Autosorb-IQ). The surface chemical compositions of the foams were examined by X-ray photoelectron spectrometer (XPS, Thermo ESCALAB 250XI) under ultrahigh vacuum (8.0×10^{-10}Pa).

2.4 Electrochemical characterization

The cyclic voltammograms (CV), galvanostatic charge-discharge, and electrochemical impedance spectroscopy (EIS) were measured on a CHI Electrochemical System (CHI660E, Shanghai ChenHua, China). A three-electrode configuration was applied during the test, with the tested foam material acting as the working electrode, a platinum wire as the counter electrode, and a saturated calomel electrode as the reference electrode. The tests were conducted in 1 M Na_2SO_4 aqueous solutions. The CV curves were collected at a scanning rate of 5 mV/s, 10 mV/s, 20 mV/s, 30 mV/s, 50 mV/s, 70 mV/s, and 100 mV/s, respectively, in the voltage window of 0-0.9 V. EIS was recorded in a frequency range of 0.01 Hz and 100 kHz at open circuit voltage with an alternate current amplitude of 5 mV. Galvanostatic charge-discharge measurements were conducted at constant current rate of 0.1 A/g, 0.5A/g, 1A/g, 2A/g, 3A/g, 5A/g and 10 A/g, respectively, with a voltage window of 0-0.9v. The specific capacitance of the test foam was calculated from the CV curve according to Eq. 1:

$$C = \frac{\int_{V_1}^{V_2} IdV}{m \times v \times (V_2 - V_1)}$$

where C (F/g) is the specific capacitance, $\int_{V_1}^{V_2} IdV$ implies area under the CV curve, m (g) is the weight of the foam block, v is the scan rate, and V_2-V_1 (V) refers to the potential window.

3. Results and Discussion

3.1 Impact of calcination temperature on the electrochemical performance of the foams

Preliminary experiments were carried out to investigate the impact of carbonization and KOH activation temperature on the electrochemical performance of the resulting foam, in order to optimize the treatment temperature for optimum double-layer capacitance behavior. The CV curves of 600-2-1-600-600 foam show a tilted thin olive shape. The tilt angel increases with an increase in the scanning rate, whereas the CV curves of ideal double-layer capacitors generally demonstrate a near-rectangular shape.[33] The results imply that 600-2-1-600-600 foam is not an ideal electrode material of double-layer supercapacitor. Compared with the CV curves of 600-2-1-600-600 foam (Fig. 1a) under similar conditions, the CV curves of 800-2-1-800-800 foam (Fig. 1b) show symmetric near-rectangular shape, a typical feature of ideal double-layer electrode materials. In contrast, the CV curves of 900-2-1-900-900 foam (Fig. 1c) shows asymmetric shape, implying that the foam is not an ideal electrode material of double-layer capacitors. Specific capacitance of three foams was calculated from the CV curves, as plotted in Fig. 1d. 600-2-1-600-600 foam, 800-2-1-800-800 foam and 900-2-1-900-900 foam displayed a specific capacitance of 35.5 F/g, 171.6 F/g and 37.5 F/g and at scan rate of 5 mV/s. The results indicate that 800-2-1-800-800 has the highest specific capacitance.
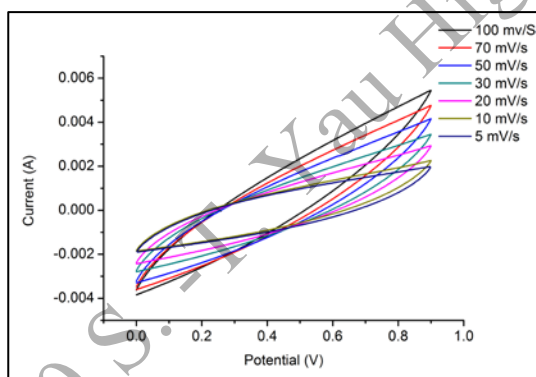
(1a) CV of 600-2-1-600-600
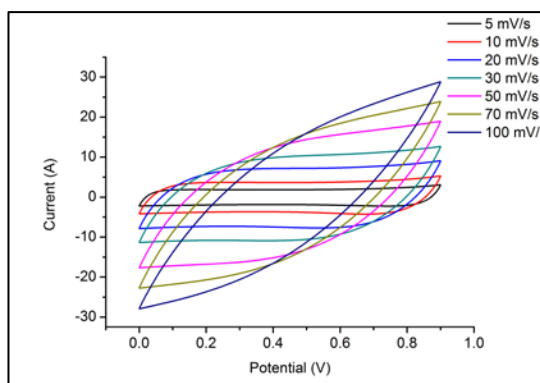
**(1b)** CV of 800-2-1-800-800
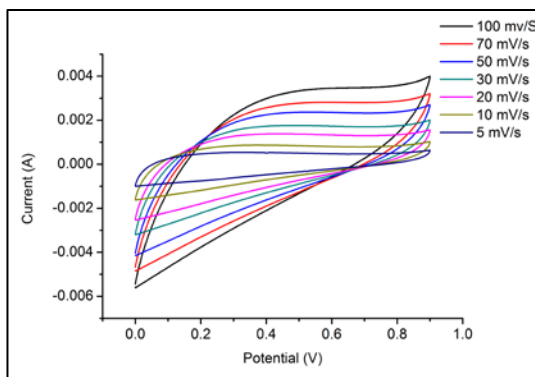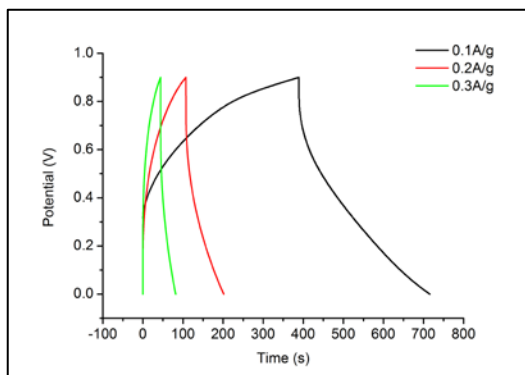
(1c) CV of 900-2-1-900-900   **(1d)** CV-calculated Specific capacitance
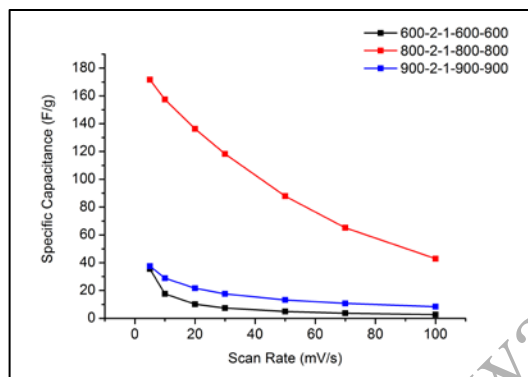
Figure 1. CV curves and specific capacitance of 600-2-1-600, 800-2-1-800-800, and 900-2-1-900-900

The kinetics of the diffusion of ion in these 3-D porous carbon foam electrodes were investigated using EIS. Fig. 2a shows the Nyquist plots of EIS obtained in 1 M Na_2SO_4 at the frequency range from 100 kHz to 0.01 Hz. The diameter of the semicircle of 600-2-1-600-600 foam is the largest, followed in descending order by 900-2-1-900-900 foam and 800-2-1-800-800 foam. The results indicate that 800-2-1-800-800 foam has the highest electric conductivity among these three foams. The near-vertical slope at low frequency region of the Nyquist plots of 800-2-1-800-800 foam manifests the rapid ionic transport in 800-2-1-800-800 electrode,[26] whereas such feature is not observed in the other two foams.
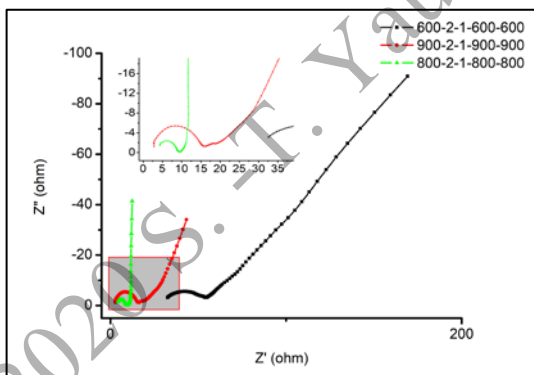
(2a) Nyquist plots of EIS   **(2b)** charge/discharge curves:600-2-1-600-600

12
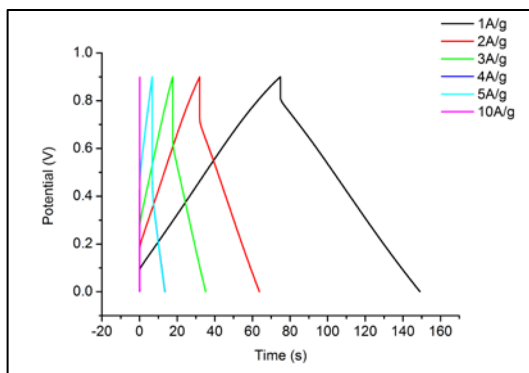
(2c) charge/discharge curves:800-2-1-800-800
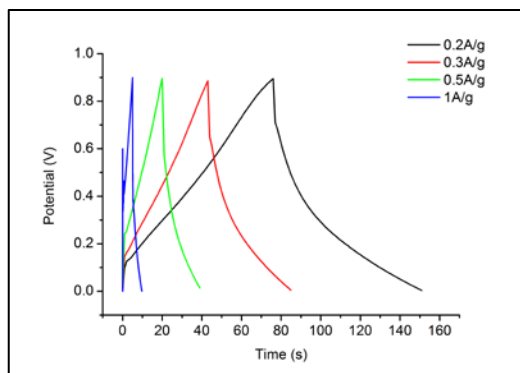
(2d) charge/discharge curves:900-2-1-900-900

Figure 2. EIS and galvanostatic charge-discharge curves of 600-2-1-600-600 foam, 800-2-1-800-800 foam and 900-2-1-900-900 foam

The galvanostatic charge-discharge curves of 600-2-1-600-600 foam, 800-2-1-800-800 foam and 900-2-1-900-900 foam are shown in Fig. 2b, Fig, 2c and Fig. 2d, respectively. The galvanostatic charge-discharge curves of 600-2-1-600-600 foam (Fig. 2b) shows nonreversible charge–discharge processes even at very low current densities (e.g. 0.5 A/g). The near symmetrical triangles of the charge/discharge plots of 800-2-1-800-800 foam (Fig. 2c) with small IR drops, especially at high current densities (e.g. 5 A/g) indicate a typical electrical double layer capacitor (EDLC) behavior of 800-2-1-800-800 foam electrode.[26] In contrast, the charge/discharge plots of 600-2-1-600-600 foam (Fig. 2b) and 900-2-1-900-900 foam (Fig. 2d) display asymmetrical triangle shape with increased IR drops, showing nonideal EDLC behavior of 600-2-1-600-600 and 900-2-1-900-900 foam electrodes.

The results of electrochemical characterization clearly indicate that 800-2-1-800-800 foam shows the most ideal double-layer capacitance behaviors. This is consistent with the substantially large specific surface area (1,555 mg^2/g) of 800-2-1-800-800 foam, whereas the specific surface areas of 600-2-1-600-600 foam (287 m^2/g) and 900-2-1-900-900 foam (181 m^2/g) are much smaller. Double-layer effect of an electrode material is directly linked to its specific surface area,[33] and the large specific area of 800-2-1-800-800 foam thus significantly contributes to its good double-layer capacitance behaviors.

13

It is known that the calcination temperature is a critical parameter for the carbonization of melamine foam,[25] the reduction of GOs,[21] the carbonization of DA and polydopamine (DPA)[30] and KOH annealing of carbon materials.[31] Higher calcination temperature facilitates carbonization of melamine, DPA and reduction of GOs, while an increase in the KOH activation temperature can enhance the surface area of the materials. However, it is observed that the foams were susceptible to destruction at elevated temperatures as well, presumably due to oxidation by trace amount of oxygen or water vapor present in the N_2 gas and excessive etching of the carbon material during KOH activation. Such weight loss of carbon materials was most significant at 900 °C, which could result in destruction of RGOs and contribute to the relatively poor electrochemical performance of 900-2-1-900-900 foam. Thus, further study was carried out with foam electrode materials prepared at a calcination temperature of 800 °C.

3.2 Impact of GOs and DA concentration on the electrochemical performance of the foams

Previous literature study indicates that the formation and the stability of GOs and DA mixed hydrogels is directly linked to the concentrations of GOs and DA as well as the ratio of GOs/DA.[27] Thus, further study was carried out to optimize the concentrations of GOs, the concentration of DA and the GOs/DA ratios. The concentrations of GOs studied were 1.0 g/L, 2.0 g/L and 10.0 g/L, while the concentrations of DA hydrochloride studied were 0.1 g/L, 0.5 g/L, 1.0 g/L and 5.0 g/L. All GOs and DA mixed solutions could develop hydrogels under the conditions studied herein. However, when the concentration of GOs was 10.0 g/L, some GOs precipitates were observed at the bottom of the flasks.

The CV curves of all foams (Figs. 3a-3e) show symmetric near-rectangular shape, typical of double-layer capacitor electrode materials. As indicated in Fig. 3f, 800-2-1-800-800 foam has the largest specific capacitance, followed in descending order by 800-10-1-800-800 foam, 800-10-5-800-800 foam, 800-2-0.5-800-800 foam, and 800-2-0.1-800-800 foam. The Nyquist plots of the EIS of the foams (Fig. 4) indicate that 800-2-1-800-800 foam has the smallest semicircle and the highest electric conductivity. The electrolyte ion has the most rapid transfer rate in 800-2-1-800-800 foam as well, as implied the near-vertical slope at

low frequency region. In addition, the galvanostatic charge-discharge curves of these foams (Fig. 5) indicate that only 800-2-1-800-800 foam (Fig. 5a) and 800-10-5-800-800 foam (Fig. 5c) show near symmetrical triangles of the charge/discharge plots. Compared with 800-10-5-800-800 foam, 800-2-1-800-800 foam displays the better charge/discharge behavior by having a longer charge and discharge time. In contrast, all the other foams show poor charge/discharge behavior, as implied by their galvanostatic charge-discharge curves (Fig. 5b, Fig. 5d and Fig. 5e).
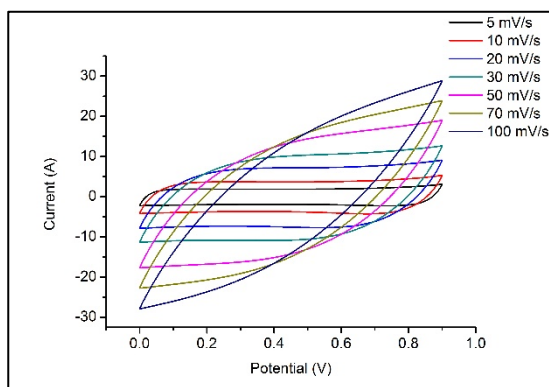
(3a) CV curves of 800-2-1-800-800
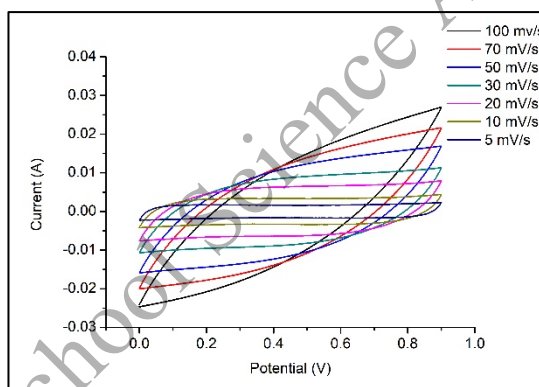
(3b) CV curves of 800-10-1-800-800
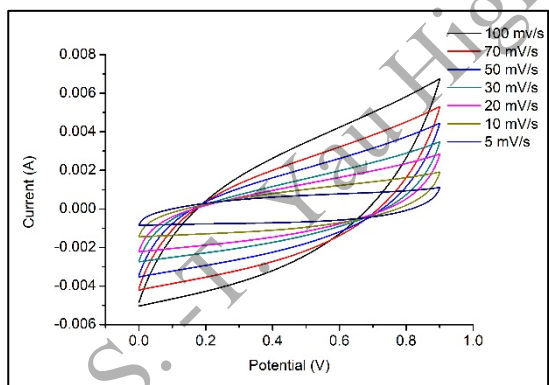
(3c) CV curves of 800-10-5-800-800
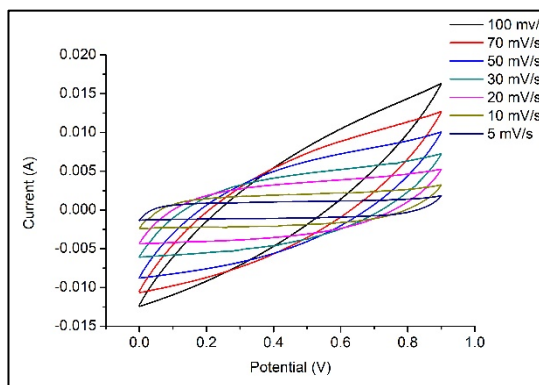
(3d) CV curves of 800-2-0.1-800-800
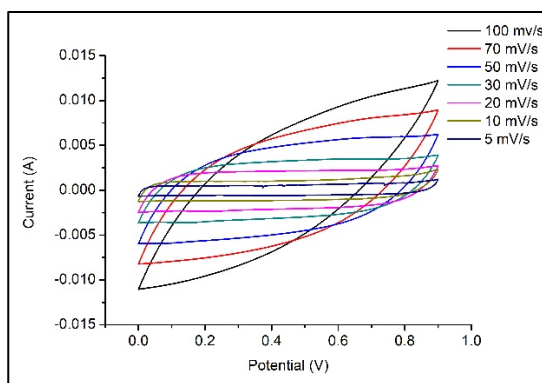
(3e) CV curves of 800-2-0.5-800-800   **(3f)** specific capacitance
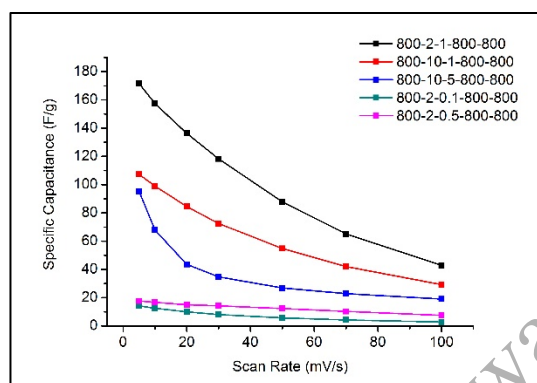
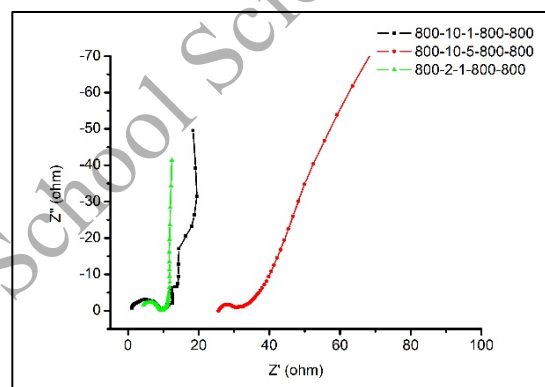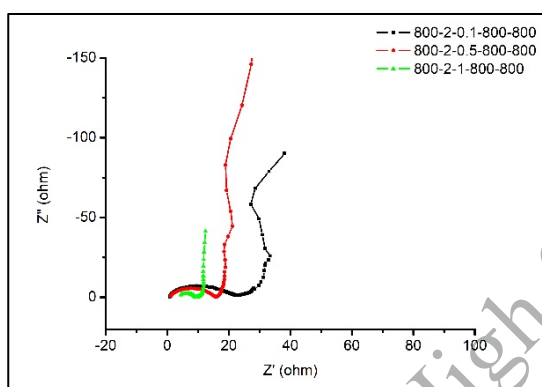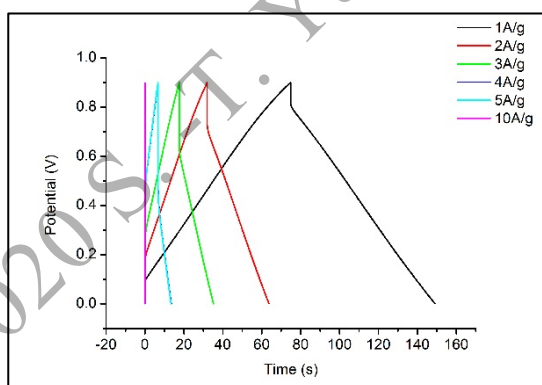**Figure 3.** Impact of GO and DA concentrations on the CV curves and specific capacitance of the foams
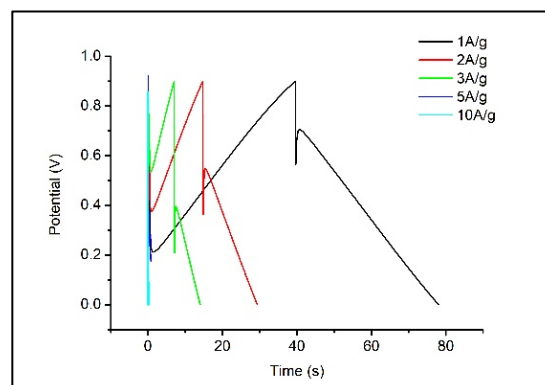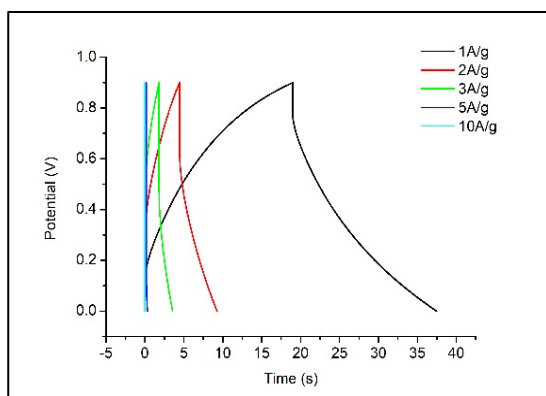

Figure 4. Impact of GO and DA concentrations on the Nyquist plots of the EIS of the foams

(5a) 800-2-1-800-800   **(5b)** 800-10-1-800-800
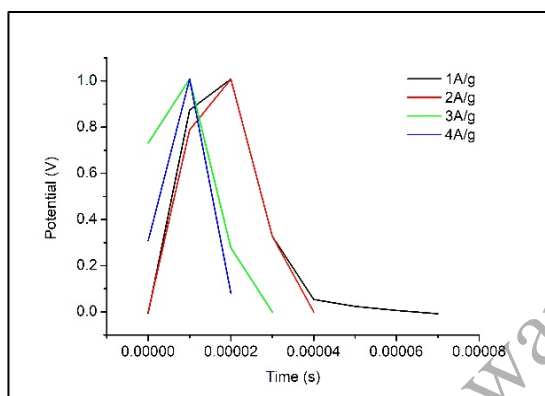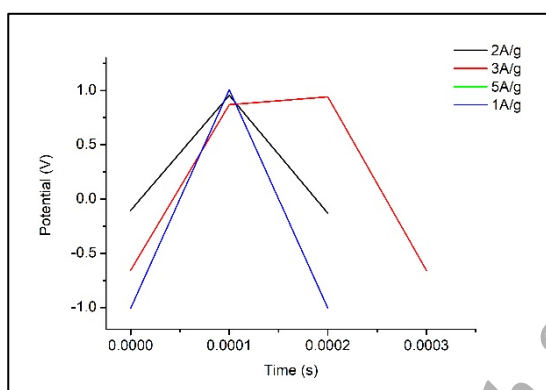
(5c) 800-10-5-800-800

(5d) 800-2-0.1-800-800


(5e) 800-2-0.5-800-800

Figure 5. Impact of GO and DA concentrations on the galvanostatic charge-discharge curves

The results of electrochemical characterization clearly indicate that 800-2-1-800-800 foam shows the most ideal double-layer capacitance behaviors. This is consistent with the largest specific surface area of 800-2-1-800-800 foam. The specific BET surface area of 800-2-1-800-800 foam is 1,555 m^2/g, followed in descending order by 800-10-1-800-800 foam (809 m^2/g), 800-10-5-800-800 foam (304 m^2/g), 800-2-0.1-800-800 foam (32 m^2/g) and 800-2-0.5-800-800 foam (18.7 m^2/g). The specific surface areas of the foams correlate with their specific capacitance very well; the larger the specific surface area, the higher the specific capacitance. This is a typical feature of double-layer capacitance material. When the concentrations of GOs were too high, clogging of the pore by GOs and precipitation of GOs might impair the entry of GOs into the pore structure. Restacking of GOs would occur to greater extent, when GO sheets precipitated out of

17

the hydrogels. On the other hand, when the concentrations of DA were too low, there was not enough DA acting as the cross-linking agent and spacer between GO sheets,[27] which could result in significant restacking of GOs as well. Based on the results, a GO concentration of 2.0 g/L and a DA hydrochloride concentration of 1.0 g/L are identified as the optimized conditions.

3.3 The loading of RGOs and KOH activation on the electrochemical performance of the foams

The optimized synthesis processes and conditions for 3-D porous nitrogen-rich carbon supported graphene foam are illustrated in Scheme 4. Commercial melamine foam is utilized as the precursor of nitrogen-rich carbon foam. Melamine foam is consisted of formaldehyde-melamine-sodium bisulfite copolymers. The foam has rich 3-D pore structure. After carbonization at 800 °C, significant shrinkage of the foam (800 foam) is observed. The 3-D pore structure can be maintained in the prepared nitrogen-rich carbon foam. It maintains high mechanical robustness, good compressibility, and provides an excellent support skeleton for GOs. The nitrogen-rich porous carbon foam (800 foam) is then immersed in aqueous solutions containing GOs and dopamine. Under optimized conditions, GOs remain well dispersed in the aqueous solutions, which allows for easy entry and loading of GOs and dopamine into the pore structure of 800 foam. Upon heating at 60 °C, black hydrogel is formed under steady conditions. This provides a convenient method to anchor and disperse GOs inside the 3-D pore structure of the foam. In addition, previous literature studies show that dopamine and GOs can be cross-linked together, which may limit the restacking of GOs.[27] To further convert GOs into RGOs and convert dopamine/polydopamine into nitrogen-doped graphene, carbonization of the GO-loaded foam at 800 °C is then carried out. The resulting foam 800-2-1-800 foam shows negligible shrinkage, and basically retains the original structure of 800 foam. 800-2-1-800 foam still maintains some level of compressibility, though the compressibility is found to reduce due to the presence of loaded RGOs and DA-derived carbonized materials inside the pore. KOH is then soaked into 800-2-1-800 foam, and annealed at high temperature 800 °C. After the treatment, the resulting 800-2-1-800-800 foam has similar structure and compressibility as 800-2-1-800 foam.
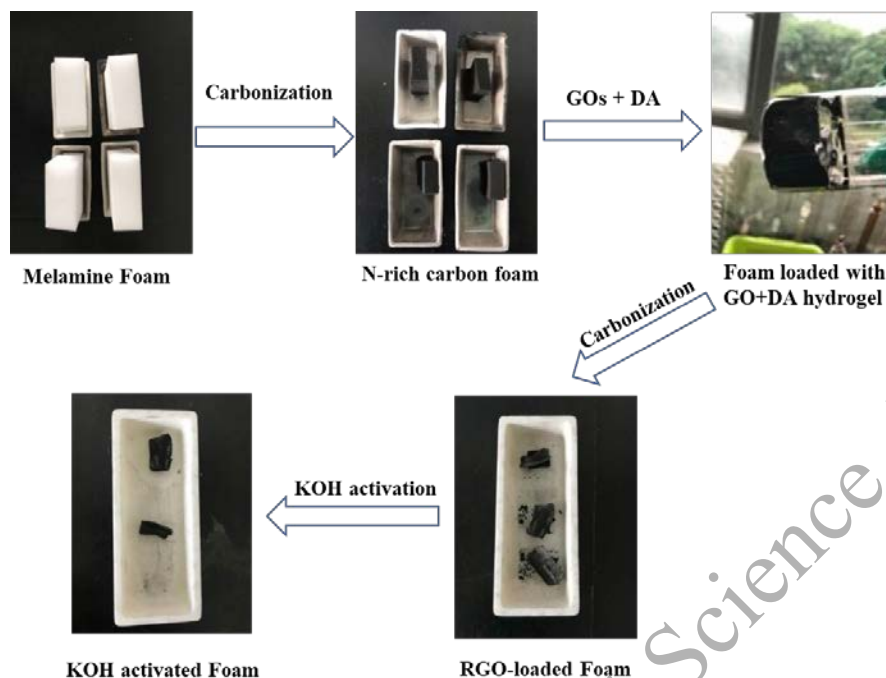
Scheme 4. Schematic illustration of the fabrication procedures for 3-D porous nitrogen-rich carbon supported reduced graphene oxide foam and corresponding digital images

SEM images of carbonized melamine foam (Fig. 6a), 800 foam show a 3-D porous network structure that is interconnected by mostly smooth branched fibers, consistent with its low BET specific area (0.27 m²/g). After 800 foam is loaded with hydrogel containing GOs and DA, SEM images of the resulting carbonized foam (Fig. 6b) indicate that the support skeleton can be retained. The pore of 800-2-1-800 is occupied by scattered flakes or sheets, presumably RGO sheets and nitrogen-rich graphene derived from dopamine/dopamine. The SEM images of 800-2-1-800-800 foams (Fig. 6b) show that RGO sheets or DA-derived graphene do not directly deposit on the surface of the fibers. RGO sheets can be further identified by the characteristic wrinkling of large RGO sheets. The results imply that the loading GO into the pore structure of 800 foam through formation of hydrogel can better disperse GO/RGOs sheet inside the pore structure while limiting the restacking of GO/RGO sheets. In addition, the RGO sheets form additional interconnected structure upon the original interconnected structure, which can further increase the electric conductivity of the foam. Due to the presence of RGO sheets and potentially DA-derived sheets, the BET

19

specific surface of 800-2-1-800 is substantially increased to 493 m^2/g. SEM image of 800-2-1-800-800 (Fig. 6c) indicate that 800-2-1-800-800 foam basically retains the 3-D porous structure of 800-2-1-800 foam. In addition, dense wrinkles and scattered holes develop on the surfaces of the support skeleton and the scattered sheets inside the pore, which thus significantly increase the BET specific surface of 800-2-1-800-800 foam (1,555 mg^2/g). The large accessible surface area and the well-developed interconnected 3-D porous structure of 800-2-1-800-800 foam are consistent with its ideal double-layer capacitor behaviors.
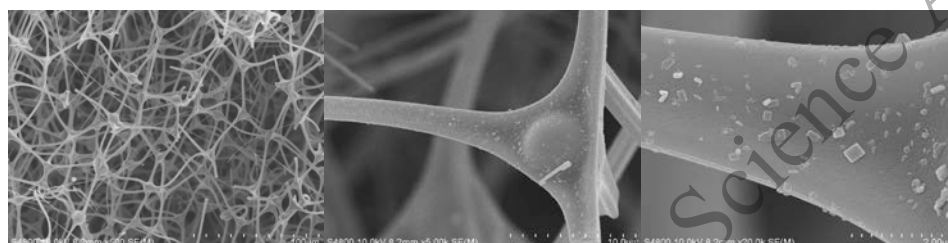

(6a) SEM images of 800 foam
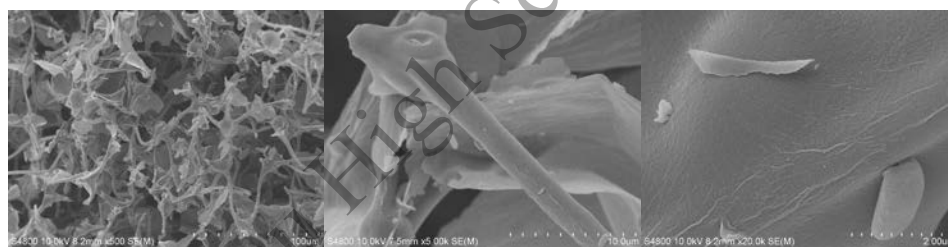
(6b) SEM images of 800-2-1-800 foam
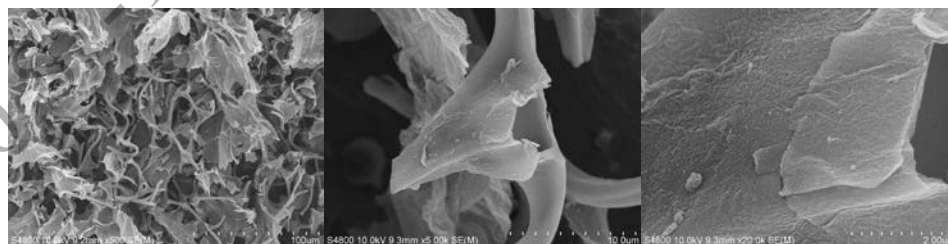
(6c) SEM images of 800-2-1-800-800

Figure 6. Impact of the loading of RGOs and KOH activation on the morphologies of the foams

20

XPS spectra of 800 foam (Fig. 7), 800-2-1-800 foam (Fig. 8) and 800-2-1-800-800 foam (Fig. 9) show the dominant existence of C peak at 285. eV, followed by the existence of N peak at 400 eV, and O peak at 533 eV. The high-resolution C1s spectra of 800 foam (Fig. 7) can be fitted into three primary components, C=C/C-C (285.0 eV), C-N/C-O (285.7 eV) and C-O-C (287.1 eV); its high-resolution N1s spectra are dominated by pydidinic-N (398.2 eV), followed by the pyrrolic-N (399.5 eV) and quternar-N/graphitic-N (400.8 eV).[26] The high-resolution O1s spectra can be fitted into four components, the quinone/pyridone-O (531.1 eV), C=O (532.5 eV), C-O-C (532.9 eV) and carboxylic-O (535.8 eV).[26] C1s spectra of 800-2-1-800 foam (Fig. 8) and 800-2-1-800-800 foam (Fig. 9) show higher proportion of C=C on their C1s spectra, compared with those of 800 foam. This is expected, as the loading of RGO and potentially nitrogen-doped graphene derived from DA/PDA into the pores of 800-2-1-800 foam and 800-2-1-800-800 foam, as both RGO and nitrogen-doped graphene consist of mostly C=C bonds. The increased proportion of quternar-N/graphitic-N component in the N1s spectra of 800-2-1-800 foam and 800-2-1-800-800 suggests increased loading of graphitic-N derived from the carbonization of DA/PDA. Increased nitrogen doping is known to improve the surface polarity and electric conductivity of the electrode material.
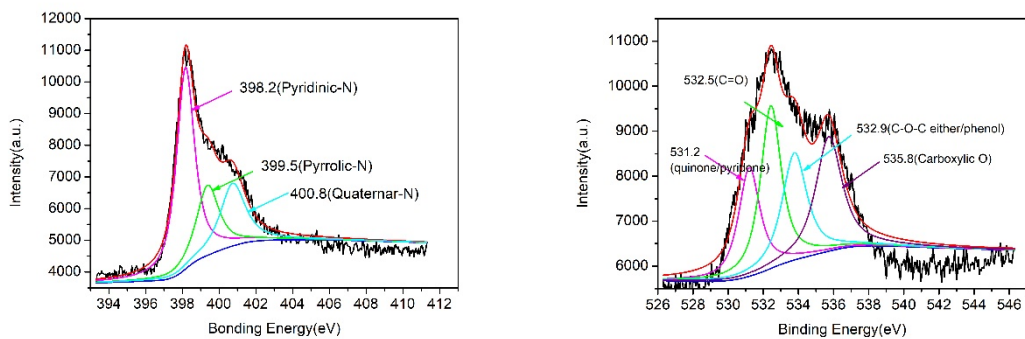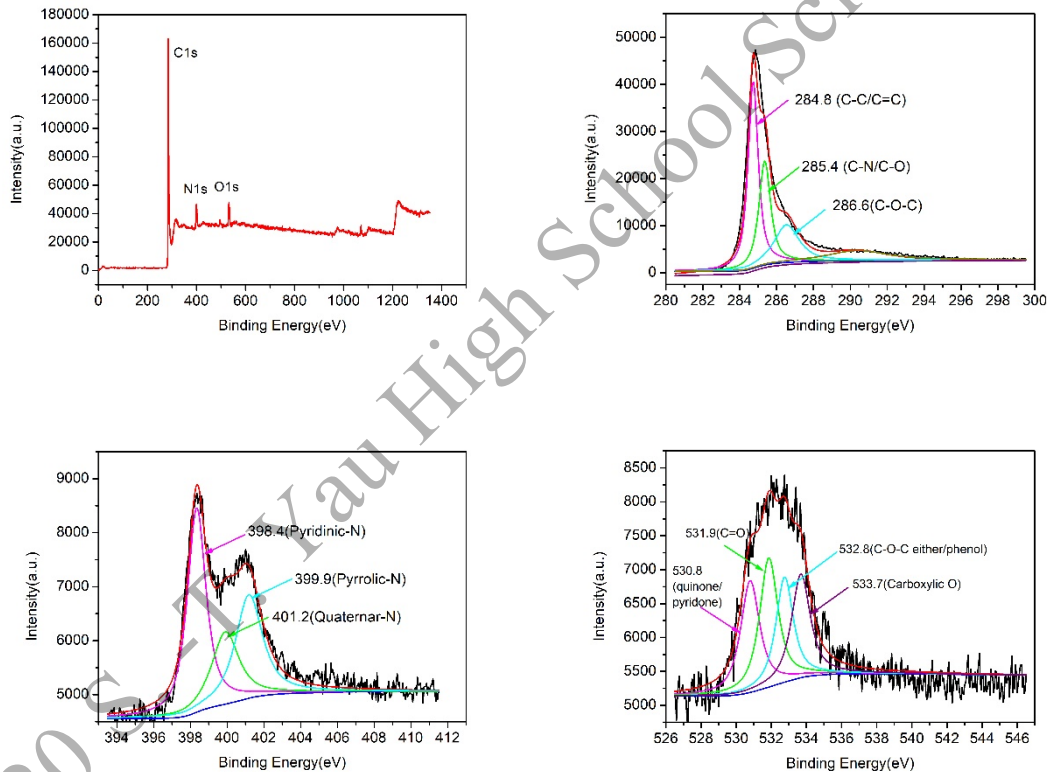

21
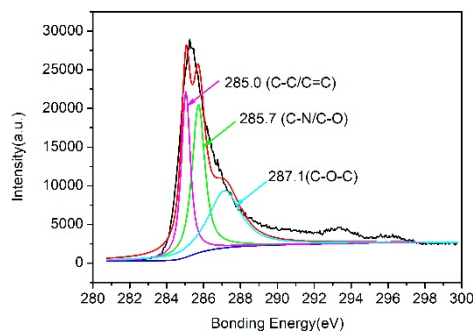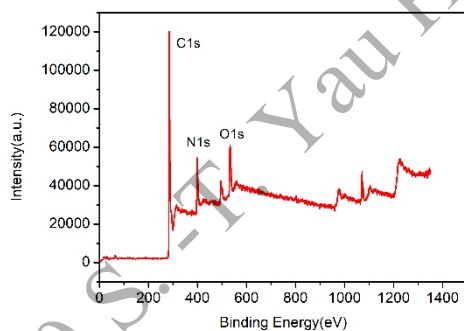
Figure 7. XPS spectra of 800 foam

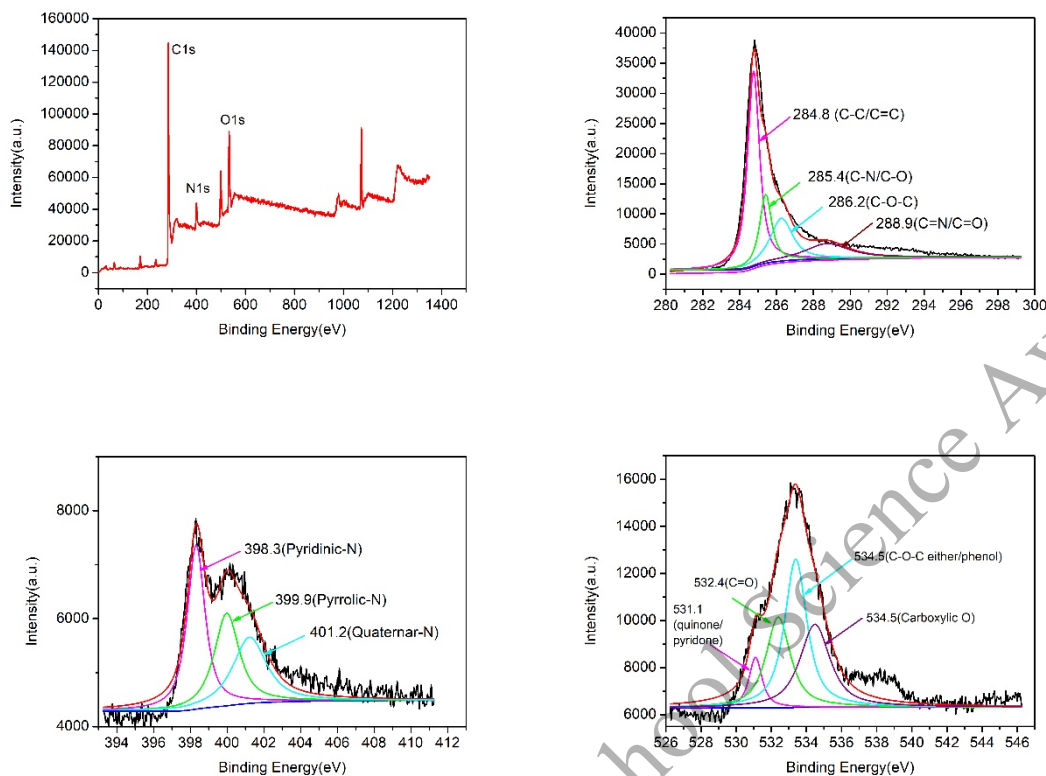**Figure 8.** XPS spectra of 800-2-1-800 foam

22

Figure 9. XPS spectra of 800-2-1-800-800 foam

The electrochemical performance of 800 foam, 800-2-1-800 foam and 800-2-1-800-800 were measured in three-electrode systems using 1 M Na_2SO_4 aqueous electrolyte. As shown in Fig. 10a-10c, the CV curves of 800 foam (Fig. 10a), 800-2-1-800 foam (Fig. 10b) and 800-2-1-800-800 foam (Fig. 10c) show a near-rectangular shapes, characteristic of typical double-layer behavior of electrode materials. The impact of scanning rate on the specific capacitance of 800 foam, 800-2-1-800 foam and 800-2-1-800-800 foam is illustrated in Fig. 10d. 800 foam, 800-2-1-800 foam and 800-2-1-800-800 foam display a specific capacitance of 6.77 F/g, 67.2 F/g and 171 .6F/g at scan rate of 5 mV/s. The results clearly indicate that both the loading of RGOs and KOH activation are critical in improving the specific capacitance of foams.
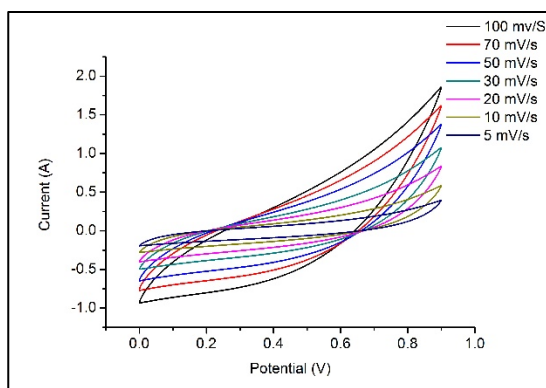
(10a) CV curves of 800
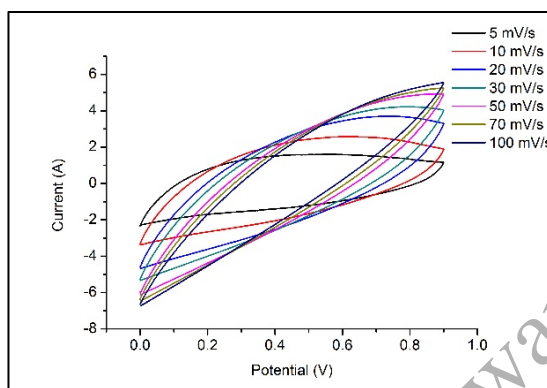
(10b) CV curves of 800-2-1-800
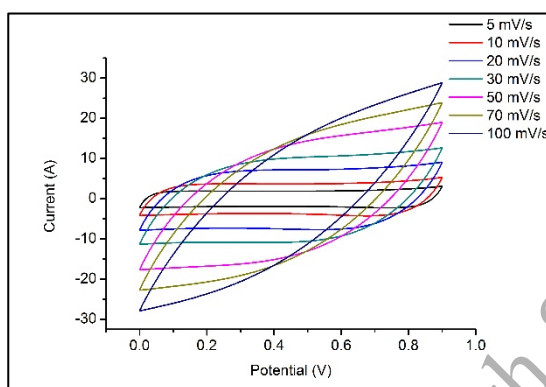
(10c) CV curves of 800-2-1-800-800
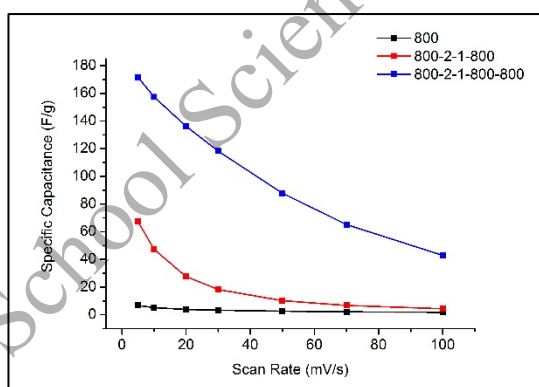
(10d) specific capacitance

Figure 10. Impact of the loading of RGOs and KOH activation on the CV curves and specific capacitance

of the foams

The kinetics of the diffusion of ion in these 3-D porous carbon foam electrodes were investigated using

EIS. Fig. 11a shows the Nyquist plot of EIS obtained in 1 M Na_2SO_4 at the frequency range from 100 kHz

to 0.01 Hz. The diameter of the semicircle of 800 foam is significantly greater than that of 800-2-1-800

foam and 800-2-1-800 foam, indicating that 800 foam has relatively poor electron transfer efficiency. In

contrast, 800-2-1-800 foam has a much smaller diameter of the semicircle. This indicate 800-2-1-800 foam

has higher electric conductivity, due to the presence of highly conductive RGOs. After KOH activation,

the semicircle of 800-2-1-800-800 foam becomes much smaller, revealing that KOH activation can

24

substantially improve the electric conductivity of 800-2-1-800-800 foam. The near-vertical slope at low frequency region of 800-2-1-800-800 foam manifests the rapid ionic transport in 800-2-1-800-800 foam, a good capacitor behavior of the material. As revealed by SEM analysis, the improved porous structure of 800-2-1-800-800 foam after KOH activation can serve as efficient mass transfer channels. At the same time, the introduced meso/micro-pores or holes in the support skeleton and RGO sheets provides increased contact surface area and convenient diffusion channels for electrolyte ions. Hence, KOH activation can substantially enhance electrolyte ions diffusion in the 3-D porous carbon foam, which are critical to high electrochemical performance.

The galvanostatic charge-discharge curves of 800 foam, 800-2-1-800 foam and 800-2-800-800 foam are shown in Fig. 11b, Fig. 11c and Fig. 11d, respectively. The galvanostatic charge-discharge curves indicate reversible charge–discharge processes with an increase in the current densities from 1 A/g to 10 A/g. However, the charge and discharge time of 800 foam and 800-2-1-800 foam is substantially less than that of 800-2-1-800-800 foam under the same conditions, consistent with the much higher specific capacitance of 800-2-1-800-800 foam. The near symmetrical triangles of the charge/discharge plots of 800-2-1-800-800 foam with small IR drops indicated a typical electrical double layer capacitor (EDLC) behavior of 800-2-1-800-800 foam. In contrast, the charge/discharge plots of 800 foam and 800-2-1-800-800 display asymmetrical triangle shape with increased IR drops, showing nonideal EDLC behaviors of 800 foam and 800-2-1-800 foam.
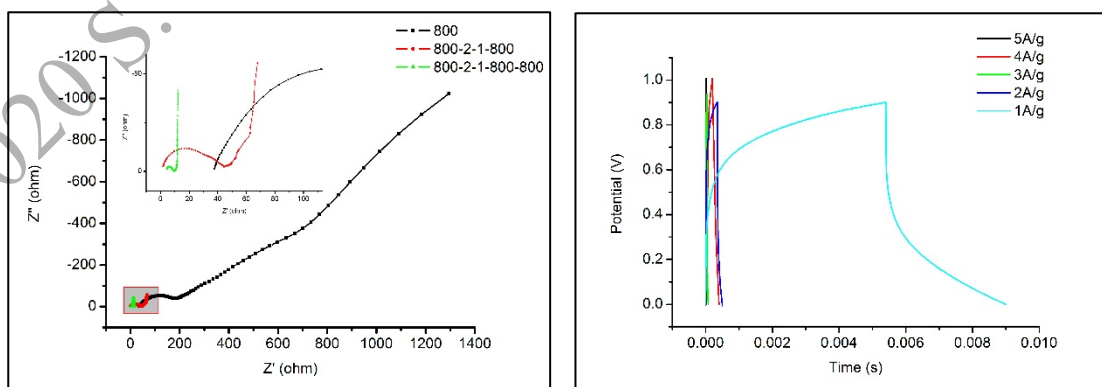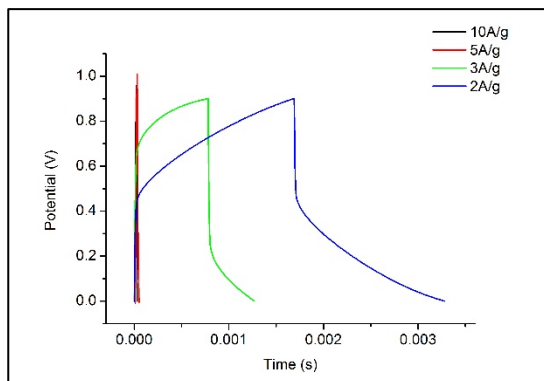
(11b) charge/discharge plots of 800 foam
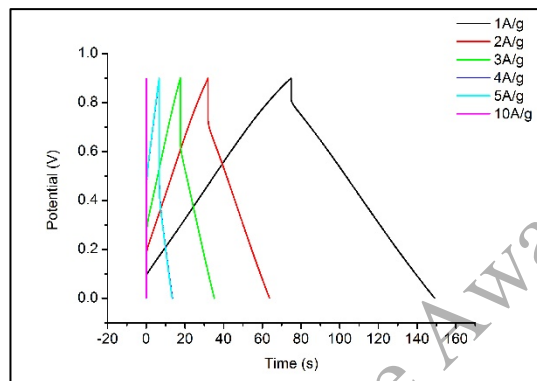
(11c) charge/discharge plots of 800-2-1-800 foam   **(11d)** charge/discharge plots of 800-2-800-800 foam

Figure 11. Impact of the loading of RGOs and KOH activation on EIS and the galvanostatic charge-discharge curves

4. Conclusions

In summary, a new synthetic route was designed and established for the preparation of 3-D graphene porous supercapacitor material. First, commercial melamine foam is carbonized at 800 °C under pure N_2 atmosphere to produce nitrogen-rich porous carbon foam as the support skeleton. Graphene oxide (GO) sheets and dopamine hydrochloride (DA) are dissolved in water, and readily dispersed into the 3-D pore structure of nitrogen-rich porous carbon foam. When heated to 60 °C, GO and DA crosslink together and form a stable hydrogel that can keep GO sheets dispersed. Thereafter, the GO loaded foam undergoes calcination under N_2 atmosphere at 800 °C to produce RGO loaded nitrogen-rich porous carbon foam. KOH activation of the RGO-loaded foam by annealing at 800 °C significantly increases the surface area and improves the electrochemical performance of the resulting final product.

The resulting foam has a large specific area (1,555 m^2/g) and a specific capacitance of 171.6 F/g at a scan rate of 5 mV/s in 1 M Na_2SO_4 aqueous solution. The specific capacitance of the 3-D RGO foam herein is

26

higher than the specific capacitance of 2-D RGO electrodes materials prepared by Stoller et al.[22] (135 F/g in KOH aqueous systems) and Yu at al.[23] (135 F/g in KCl aqueous systems). The results imply that the prepared 3-D RGO foam has exceptional specific capacitance, comparable to the 3-D RGO foam prepared by Xu et al.[24] (165 F/g), though it should be cautious to directly compare the specific capacitance of these RGO materials due to the various test conditions used. SEM analysis shows that the final foam product has 3-D pore structure with RGO sheets dispersed in the pore space, and the restacking issue can be minimized through optimization of the concentrations of GO and DA. Overall, this study develops a promising process for the fabrication of porous nitrogen-rich carbon supported 3-D reduced graphene oxide foam as high-performance supercapacitor electrodes.

Further investigation is currently being carried out to measure the pore volume and pore size distribution of the material and explore how the microstructure of the foam regulates the electrochemical performance of the foam. Further optimization of the electrochemical properties of the 3-D reduced graphene oxide foam is also being planned in future studies, followed by fabrication of supercapacitor devices to test the applicability of the foam as well.

References

[1] J.R. Miller, P. Simon, Electrochemical Capacitors for Energy Management, Science, 321 (2008) 651-652.

[2] G. Wang, L. Zhang, J. Zhang, A review of electrode materials for electrochemical supercapacitors, Chemical Society Reviews, 41 (2012) 797-828.

[3] R. Kötz, M. Carlen, Principles and applications of electrochemical capacitors, Electrochimica Acta, 45 (2000) 2483-2498.

[4] E. Frackowiak, F. Béguin, Carbon materials for the electrochemical storage of energy in capacitors, Carbon, 39 (2001) 937-950.

[5] P. Simon, Y. Gogotsi, Materials for electrochemical capacitors, Nature Materials, 7 (2008) 845-854.

[6] M. Vangari, T. Pryor, L. Jiang, Supercapacitors: Review of Materials and Fabrication Methods, Journal of Energy Engineering, 139 (2013) 72-79.

[7] B.E. Conway, V. Birss, J. Wojtowicz, The role and utilization of pseudocapacitance for energy storage by supercapacitors, Journal of Power Sources, 66 (1997) 1-14.

[8] T. Guo, D. Zhou, W. Liu, J. Su, Recent advances in all-in-one flexible supercapacitors, Science China-Materials, (2020).

[9] Z. Lin, Z. Zeng, X. Gui, Z. Tang, M. Zou, A. Cao, Carbon Nanotube Sponges, Aerogels, and Hierarchical Composites: Synthesis, Properties, and Energy Applications, Advanced Energy Materials, 6 (2016).

[10] L. Liu, Z. Niu, J. Chen, Flexible supercapacitors based on carbon nanotubes, Chinese Chemical Letters, 29 (2018) 571-581.

[11] F. Liu, G. Han, Y. Chang, D. Fu, Y. Li, M. Li, Fabrication of Carbon Nanotubes/Polypyrrole/Carbon Nanotubes/Melamine Foam for Supercapacitor, Journal of Applied Polymer Science, 131 (2014).

[12] Y. Chen, G.Z. Chen, New Precursors Derived Activated Carbon and Graphene for Aqueous Supercapacitors with Unequal Electrode Capacitances, Acta Physico-Chimica Sinica, 36 (2020).

[13] A. Kausar, Advances in polymer-anchored carbon nanotube foam: a review, Polymer-Plastics Technology and Materials, 58 (2019) 1965-1978.

[14] L. Lin, H. Ning, S. Song, C. Xu, N. Hu, Flexible electrochemical energy storage: The role of composite materials, Composites Science and Technology, 192 (2020).

[15] S. Venkateshalu, A.N. Grace, Review-Heterogeneous 3D Graphene Derivatives for Supercapacitors, Journal of the Electrochemical Society, 167 (2020).

[16] Q. Ke, J. Wang, Graphene-based materials for supercapacitor electrodes – A review, Journal of Materiomics, 2 (2016) 37-54.

[17] Y. Gao, Graphene and Polymer Composites for Supercapacitor Applications: a Review, Nanoscale Research Letters, 12 (2017) 387.

[18] M. Horn, B. Gupta, J. MacLeod, J. Liu, N. Motta, Graphene-based supercapacitor electrodes: Addressing challenges in mechanisms and materials, Current Opinion in Green and Sustainable Chemistry, 17 (2019) 42-48.

[19] E. Lai, X. Yue, W.e. Ning, J. Huang, X. Ling, H. Lin, Three-Dimensional Graphene-Based Composite Hydrogel Materials for Flexible Supercapacitor Electrodes, Frontiers in Chemistry, 7 (2019).

[20] J. Liu, Y. Zeng, J. Zhang, H. Zhang, J. Liu, Preparation, Structures and Properties of Three-Dimensional Graphene-Based Materials, Progress in Chemistry, 31 (2019) 667-680.

[21] S. Pei, H.-M. Cheng, The reduction of graphene oxide, Carbon, 50 (2012) 3210-3228.

[22] M.D. Stoller, S. Park, Y. Zhu, J. An, R.S. Ruoff, Graphene-Based Ultracapacitors, Nano Letters, 8 (2008) 3498-3502.

[23] A.P. Yu, I. Roes, A. Davies, Z.W. Chen, Ultrathin, transparent, and flexible graphene films for supercapacitor application, Appl. Phys. Lett., 96 (2010) 3.

[24] Y. Xu, K. Sheng, C. Li, G. Shi, Self-Assembled Graphene Hydrogel via a One-Step Hydrothermal Process, Acs Nano, 4 (2010) 4324-4330.

[25] Y. Shi, G. Liu, R. Jin, H. Xu, Q. Wang, S. Gao, Carbon materials from melamine sponges for supercapacitors and lithium battery electrode materials: A review, Carbon Energy, 1 (2019) 253-275.

[26] R. Tjandra, W.W. Liu, L. Lim, A.P. Yu, Melamine based, n-doped carbon/reduced graphene oxide composite foam for Li-ion Hybrid Supercapacitors, Carbon, 129 (2018) 152-158.

[27] H.C. Gao, Y.M. Sun, J.J. Zhou, R. Xu, H.W. Duan, Mussel-Inspired Synthesis of Polydopamine-Functionalized Graphene Hydrogel as Reusable Adsorbents for Water Purification, ACS Appl. Mater. Interfaces, 5 (2013) 425-432.

[28] L. Han, X. Lu, M. Wang, D. Gan, W. Deng, K. Wang, L. Fang, K. Liu, C.W. Chan, Y. Tang, L.-T. Weng, H. Yuan, A Mussel-Inspired Conductive, Self-Adhesive, and Self-Healable Tough Hydrogel as Cell Stimulators and Implantable Bioelectronics, Small, 13 (2017).

[29] L.Q. Xu, W.J. Yang, K.G. Neoh, E.T. Kang, G.D. Fu, Dopamine-Induced Reduction and Functionalization of Graphene Oxide Nanosheets, Macromolecules, 43 (2010) 8336-8339.

[30] J. Wang, Y. Zeng, L.L. Wan, J.Y. Zhao, J. Yang, J. Hu, F.F. Miao, W.T. Zhan, R.S. Chen, F. Liang, Catalyst-free fabrication of one-dimensional N-doped carbon coated TiO2 nanotube arrays by template carbonization of polydopamine for high performance electrochemical sensors, Appl. Surf. Sci., 509 (2020) 8.

[31] J.C. Wang, S. Kaskel, KOH activation of carbon-based materials for energy storage, J. Mater. Chem., 22 (2012) 23710-23725.

[32] Y. Chen, X. Qiu, L.-Z. Fan, Nitrogen-rich hierarchically porous carbon foams as high-performance electrodes for lithium-based dual-ion capacitor, Journal of Energy Chemistry, 48 (2020) 187-194.

[33] E. Frackowiak, F. Beguin, Carbon materials for the electrochemical storage of energy in capacitors, Carbon, 39 (2001) 937-950.

29

Acknowledgements

The author would like to appreciate the guidance and instructions of Xiaoan Yang and Pro. Dayi Deng for their valuable guidance. Most of the experiments were carried out in the School of Environment of South China Normal University, and the author is thankful to Prof. Deng's group for kindly offering space and instruments for the study.

Resume of Team Member

Runnan Hong

The Affiliated High School of SCNU, Guangzhou, 510630, P.R. China

Tel: 15626490369

Email: 842473715@qq.com

Personal Data:

Sex: Male Date of Birth: May 25

Birthplace: Guangzhou, Guangdong Province, P.R. China

Resume of Instructors

Dr. Dayi Deng

Associate Professor, School of Environment, South China Normal University, Guangzhou, P.R. China

Tel: 020-3931-0213

Email: dengdayi@scnu.edu.cn

Dr. Dayi Deng graduated from the Chemistry Department of Princeton University in 2007 with a PhD. Thereafter, he worked as a Senior Environmental Chemist for FMC Corporation (NJ, USA) from Feb. 2007 to Feb. 2010. After March 2010, Dr. Deng returned to China and joined South China Normal University as a faculty member.

Xiaoan Yang

The Affiliated High School of South China Normal University, Guangzhou, Guangdong, P.R. China

Tel: 18902266906

Email: 18902266906@189.cn

Xiaoan Yang, Senior Teacher of the Attached Middle School of South China Normal University, is currently head of the Steering Group for Student Research Activities. He has been appointed the counselor of the school's Youth Science and Technology Innovation Program since 2000. He won the top teacher's prize of the 4th China Association of Science and Technology Science and Technology Innovation Talent Training Project (only 10 teachers national-wide), the Gardener Award of the 9th Guangdong Children's Invention Award in 2009, the Gardener Award of the 6th Song Qingling Children's Invention Award, etc.